HHS Public Access

Author manuscript

Proc SPIE Int Soc Opt Eng. Author manuscript; available in PMC 2015 May 27.

Published in final edited form as:

Proc SPIE Int Soc Opt Eng. 2011 January 22; 7886: . doi:10.1117/12.873337.

Investigating the photosensitizer-potential of targeted gallium corrole using multimode optical imaging

Jae Youn Hwang[a], **Jay Lubow**[a], **David Chu**[a], **Zeev Gross**[e,f], **Harry B. Gray**[e], **Daniel L. Farkas**[c,d], and **Lali K. Medina-Kauwe**[a,b]

[a]Department of Biomedical Sciences, Cedars-Sinai Medical Center, Los Angeles, CA

[b]Geffen School of Medicine, University of California Los Angeles, Los Angeles, CA

[c]Department of Biomedical Engineering, University of Southern California, Los Angeles, CA

[d]Spectral Molecular Imaging, Inc., Beverly Hills CA

[e]Beckman Research Institute, California Institute of Technology, Pasadena, CA

[f]Department of Chemistry, Technion-Israel Institute of Technology, Haifa

Abstract

We recently developed a novel therapeutic particle, HerGa, for breast cancer treatment and detection. HerGa consists of a tumor-targeted cell penetration protein noncovalently assembled with a gallium-metallated corrole. The corrole is structurally similar to porphyrin, emits intense fluorescence, and has proven highly effective for breast tumor treatment preclinically, without light exposure. Here, we tested HerGa as a photosensitizer for photodynamic therapy and investigated its mechanism of action using multimode optical imaging. Using confocal fluorescence imaging, we observed that HerGa disrupts the mitochondrial membrane potential *in situ*, and this disruption is substantially augmented by light exposure. In addition, spectral and fluorescence lifetime imaging were utilized to both validate the mitochondrial membrane potential disruption and investigate HerGa internalization, allowing us to optimize the timing for light dosimetry. We observed, using advanced multimode optical imaging, that light at a specific wavelength promotes HerGa cytotoxicity, which is likely to cause disruption of mitochondrial function. Thus, we can identify for the first time the capacity of HerGa as a photosensitizer for photodynamic therapy and reveal its mechanism of action, opening possibilities for therapeutic intervention in human breast cancer management.

Keywords

Multimode optical imaging; targeted gallium corrole; photosensitizers; spectral imaging; fluorescence lifetime imaging

Correspondence to: Daniel L. Farkas; Lali K. Medina-Kauwe.

1. INTRODUCTION

Porphyrin-like compounds have been widely used as photosensitizers in photodynamic therapy for various disease treatments (1, 2). In particular, several compounds, including Photofrin, Levulan, and Metvix, are already being used in the clinic for lung, esophageal, and bladder cancer treatment (3–5). However, corroles, which are macrocyclic compounds with a porphyrin-like structure, have not been thoroughly explored in biological systems until our own recent studies *in vitro* (6, 7) and *in vivo* (8). We have shown that the particle, HerGa, comprised of sulfonated gallium-metallated corrole (S2Ga) complexed with the recombinant tumor-targeted cell penetrating protein, HerPBK10, is highly effective for tumor detection and treatment in an animal model of HER2+ breast cancer, which is a highly aggressive breast cancer that resists standard treatment. In addition, these studies revealed that HerPBK10 is non-immunogenic and facilitates the targeted systemic delivery of S2Ga to tumor cells *in vivo* through human epidermal growth factor receptor (HER) ligation, endocytosis, and endosomal penetration, enabling corrole-mediated cell killing (6). HerGa self-assembles non-covalently while exhibiting high stability in serum. Unlike trastuzumab, HerPBK10 contains the receptor binding domain of heregulin, which has an enhanced affinity for tumors displaying elevated HER subunit 2 (HER2) but does not directly interact with HER2, thus avoiding tissue displaying normal HER2 levels (such as the heart), and hence indicating that HerGa may present an improved alternative strategy for HER2+ tumor killing compared to current targeted therapies (9–11).

Whereas HerGa is structurally similar to porphyrins (3–5), its photosensitizing potential has not been fully investigated, thus prompting an exploration of this possibility in the current study. Here we used multimode optical imaging, including bright-field, fluorescence confocal, spectral, and lifetime imaging (6), to show that HerGa exhibits photosensitizer properties that augment its inherent cytotoxicity. This additional capability may enhance the potency and specificity of the drug for tumor treatment by combining with the inherent cytotoxicity of HerGa, thus further reducing drug dosage and consequently possible side-effects, as well as resulting in rapid translation into clinical use (1, 2).

In this investigation, we apply multiple imaging techniques (including bright-field, fluorescence confocal, spectral, and lifetime imaging) that offer complementary and synergetic information in identifying the characteristics of molecules and their mechanism, resulting in eliminating potential blind spots, which can not ordinarily be detected using a single imaging mode (6). These studies examine the effect of HerGa on mitochondrial membrane potential in MDA-MB-435 cells -/+ light exposure by measuring the mitochondrial accumulation of a cationic fluorescent probe, tetramethyl rhodamine, methyl ester (TMRM) using confocal, bright-field, and spectral imaging. In addition, we examined HerGa uptake using fluorescence lifetime imaging in order to determine the optimal timing for light dosimetry on the cells.

2. METHODS AND MATERIALS

2.1 Materials

MDA-MB-435 cells (National Cancer Institute) were cultured in Dulbecco's modified Eagle's Medium (DMEM) supplemented with 10% fetal bovine serum and penicillin/streptomycin at 37° C, 5% CO_2. HerGa was produced through non-covalently binding of HerPBK10 protein, which was expressed in *Escherichia coli* as a histidine-tagged fusion protein and purified by metal chelate affinity chromatography, to S2Ga at a molar ratio of 30:1 as previously described (7). TMRM was obtained from Invitrogen.

2.2 Experimental setup for multimode optical imaging

A Leica TCS SPE confocal and a Nikon TE 2000 microscope were used for multimode optical imaging. The Leica confocal imaging system was used for bright-field, confocal, and spectral imaging while the Nikon TE 2000 microscope, which is modified to connect multiple imaging devices (up to 4 devices) and deliver versatile laser lines, was utilized for fluorescence lifetime measurement. For live cell imaging, a delta T chamber was utilized in order to control temperature during image acquisition. A temperature-controlled stage integrated with the microscopes was used to control the temperature of samples.

Mitochondrial damage by HerGa -/+ light was assessed by bright-field, confocal, and spectral imaging of the MDA-MB- 435 cells sequentially. 405nm and 535nm laser light were delivered to the samples through an objective (63x, NA: 1.3, Leica) for excitation of HerGa and TMRM respectively. The emitted light from the samples was filtered by a light wavelength selector, and then recorded in photomultiplier tubes (PMT). To discriminate between HerGa and TMRM fluorescence, thirteen images were acquired within the spectral range (530–650nm, with a step size, 10nm) for the spectral imaging and analysis, and then the images were analyzed using the spectral classification program we previously developed (12). Bright-field imaging, used to monitor morphological changes of the cells, was performed sequentially using the transmission mode of the Leica system [Fig. 1.(A)].

For fluorescence lifetime imaging, femtosecond (fs) pulsed laser light (100fs) tuned to 424nm, at a repetition rate of 80MHz, generated by the second harmonic of fs pulsed laser at 848nm in a Beta Barium Borate (BBO) crystal, was delivered to the Nikon Microscope through macro lenses, a band-pass filter (425±5nm), several mirrors, and a diffuser. The delivered light was reflected to the back focal plane of a 100x objective (Nikon 100x planfluor, NA: 1.3) for the excitation of HerGa. The fluorescence from HerGa was collected by the objective and recorded in the CCD connected with the time-gated intensifier (TGI) (Lavison) through an emission filter (620±60nm). The CCD and the time-gated intensifier were synchronized with pulsed light via a delay unit that connects with the external trigger [Figure 1.(B)].

2.3 Mitochondrial membrane potential measurement

TMRM is a cationic dye used to measure mitochondrial membrane potential in live cells. Its distribution across the mitochondrial membrane is governed primarily by the Nernst equation (13). To measure the mitochondrial membrane potential of HerGa treated cells -/+

light, 10^4 MDA-MB-435 cells were plated at four Delta T chambers and incubated for 36 hours, and then media was aspirated from each chamber and replaced with 1ml DMEM supplemented with 10% fetal bovine serum and penicillin/streptomycin containing either 1μM HerGa, 1μM S2Ga, HerPBK10 (at equivalent protein concentration as HerGa), or PBS at 37° C, 5% CO_2. After the 24 hours, the media in the chambers was aspirated and replaced with 20nM TMRM diluted with HBSS, and then confocal TMRM fluorescence images were acquired -/+ light exposure (450nm–490nm, 17J/cm^2) at different z-depths after the equilibrium of TMRM accumulation in the cells (~ 1 hour).

3. RESULTS

3.1 Confocal, bright-field and spectral imaging allow monitoring variations of mitochondrial membrane permeability by HerGa-mediated photosensitization, quantitatively

To assess whether HerGa possesses photosensitizer activity, both mitochondrial membrane permeability and morphologic changes (indicating cellular health status) of MDA-MB-435 cells, confocal/bright-field/spectral imaging was performed after treatment with HerGa and other control molecules -/+ light exposure. Specifically, cells growing in delta T chambers were treated with 1μM HerGa, 1μM S2Ga, PBS, and HerPBK10 for 24 hours before addition of TMRM and TMRM fluorescence, bright-field, and spectral classified images were acquired sequentially [Fig. 2.] (14). In Figure 2.(A), without light exposure, there is still detectable TMRM accumulation in mitochondria and the cells exhibit similar morphology to that of healthy cells. However, after the light exposure, mitochondrial accumulation of TMRM is dramatically reduced while the cells exhibit a rounded, cytopathic morphology. Spectral imaging, which enables discrimination between HerGa and TMRM fluorescence signals quantitatively, was additionally performed -/+ light exposure. The spectral classification images, created by the spectral classification program we developed previously (12), show that after the light exposure, while HerGa (green pseudo-color) is indeed accumulated diffusely inside cells that have undergone mitochondrial disruption, TMRM (red pseudo-color) appears diffused away from mitochondria into the cytoplasm and outside cells. Figure 2.(B) shows the results for the control experiment. Unlike Figure 2.(A), the mitochondrial membrane potential variations in control-treated cells -/+ light exposure were much less than in the HerGa-treated cells [Fig.2. (B)]. Taken together, these results show that the bright-field/confocal/spectral imaging allows us to monitor the mitochondrial membrane permeability and morphologic changes of the HerGa treated cells -/+light quantitatively and specifically, thus revealing toxic properties of HerGa that are activated by photoexcitation.

3.2 Fluorescence lifetime changes of HerGa during internalization into MDA-MB-435 cells

The results shown in Figure 2 indicate that light at specific wavelengths can promote mitochondrial damage in HerGa-treated cells, but not significantly in S2Ga-treated cells, in which cellular uptake of S2Ga is much less than HerGa (8). The results suggest that cell entry is required for HerGa-mediated photosensitization, and indicate that light exposure should occur some time after the internalization of HerGa in order to induce its photosensitizing effect efficiently. Our previous studies show that HerPBK10-mediated

delivery yields accumulation in endocytic vesicles by 15 min after uptake followed by sufficient cytosolic distribution of HerPBK10 by 45 min (8). Hence, we examined whether HerGa fluorescence lifetime could be used as a live-cell indicator to signal the optimal timing for light exposure within this established time window of uptake. Figure 3 shows the fluorescence lifetime and intensity images of HerGa, which were obtained at the indicated time-points after the cells were exposed to 25 μM HerGa, during uptake. A higher than normal concentration of HerGa was used here to provide high signal to noise ratio for adequate fluorescence lifetime detection. In the Figure 3.(A), while the average fluorescence lifetime of HerGa on the cells is approximately 0.87ns (0.64~1.03ns) at 3 minutes, the average fluorescence lifetime of HerGa decreases to approximately 0.55ns at 30 minutes. Interestingly, the fluorescence lifetimes of HerGa (average: 0.58ns) at 60 minutes somewhat increases, but not significantly compared to at 30 minutes. This increase is likely to reflect the endosomal escape of HerGa, as cytosolic distribution takes place by 45 min after cell entry (8). The histograms [Fig. 3.(B)] detail the distribution of fluorescence lifetimes of HerGa. At 3 minutes, the histogram has peaks at 0.84ns and 0.94ns. The fluorescence lifetimes are of relatively low frequency below 0.8ns. On the other hand, the peaks at 30 and 60 minutes are shifted to around 0.48 ns and 0.53ns respectively. Finally, the fluorescence intensity images show that while HerGa accumulates on cell membrane at 3 minutes, it is localized in the cytoplasm while remaining excluded from the nucleus after 30 minutes [Fig. 3. (C)]. Altogether, these results show that initial HerGa uptake is realized within 30 minutes after the addition of HerGa onto the cells, thus allowing us to identify the optimal timing for inducing photoexcitation. Moreover, the fluorescence lifetime imaging enables us to monitor intracellular micro-environmental changes encountered during HerGa uptake, including those changes characterizing endosomal escape.

4. DISCUSSION AND CONCLUSIONS

The mitochondrion is a common target for many photosensitizers (15, 16) and monitoring its membrane potential can be a powerful approach for identifying the toxic activity of various drugs (6, 17). Our present studies show that HerGa similarly causes mitochondrial membrane potential disruption through modulation by photoexcitation, and the multimode imaging used here allows us to characterize the events surrounding this activity intracellularly, in real-time, and in live cells. Similar to other photosensitizers, HerGa requires membrane penetration to damage cells. This is provided by the endosomolytic domain of HerPBK10, which is shown elsewhere to facilitate cytosolic delivery of corroles and nucleic acids (6–8). In agreement, Figure 2 shows that corrole-mediated cell damage induced by photoexcitation occurs when S2Ga is delivered by HerPBK10 (in other words, by fully assembled HerGa), but not by HerPBK10 or S2Ga alone.

Fluorescence lifetime imaging also enables us to characterize HerGa cell entry in real-time. Figure 3 shows that the fluorescence lifetimes of HerGa decrease as it is internalized into the cells. As our previous studies indicate that HerPBK10-mediated cell entry occurs by receptor-mediated endocytosis and endosomal escape (6, 7), the fluorescence lifetime changes of HerGa during uptake may reflect intracellular microenvironmental changes encountered during its transit. Particularly, the fluorescence lifetime increase of HerGa after 30 minutes may reflect the endosomal escape of HerGa. As the microenviroment of the

cytosol is less acidic than in endosomal vesicles, this could be indicative of pH changes, though this remains to be elucidated.

In conclusion, these studies reveal that in addition to its reported inherent cytotoxicity (6, 7), HerGa also has photosensitizer activity that may augment its tumor-toxic potency. The multimode optical imaging used in the identification of the photosensitizer activity of HerGa and its mechanism of mitochondrial damage has also enabled realtime characterization of the HerGa intracellular microenvironment during uptake. Thus, the multimode optical imaging has allowed the acquisition of complementary information that is not obtainable through single-mode imaging. Meanwhile, the combination of the inherent tumor-toxicity of HerGa and its newly discovered photo-reactivity may enable even greater potency and specificity for killing tumor cells, thus yielding a therapeutic with optimized efficacy and safety.

ACKNOWLEDGEMENTS

This work was supported by grants from the NIH (R21 CA116014, R01 CA102126, R01 CA129822, and R01 CA140995), the DoD (BC050662), the Susan G. Komen Breast Cancer foundation (BCTR0201194), and the Donna and Jesse Garber Award. Work at Caltech was supported by NIH DK019038 and the Arnold and Mabel Beckman Foundation. Work at the Technion was supported by The Herbert Irving Cancer and Atherosclerosis Research Fund. Partial support from the US Navy Bureau of Medicine and Surgery is gratefully acknowledged. LKMK wishes to thank JC, MMK, and DR for ongoing support.

REFERENCES

1. Dougherty TJ, Gomer CJ, Henderson BW, Jori G, Kessel D, Korbelik M, Moan J, Peng Q. Photodynamic therapy. J. Natl. Cancer. Inst. 1998; 90:889–905. [PubMed: 9637138]
2. Via LD, Magno SM. Photochemotherapy in the treatment of cancer. Curr. Med. Chem. 2001; 8:1405–1418. [PubMed: 11562274]
3. Juarranz A, Jaen P, Sanz-Rodriguez F, Cuevas J, Gonzalez S. Photodynamic therapy of cancer. Basic principles and applications. Clin Transl Oncol. 2008; 10(3):148–154. [PubMed: 18321817]
4. Zimcik P, Miletin M. Photodynamic therapy as a new prospective method for cancer treatment. I. History, basic principles. Ceska Slov Farm. 2004; 53(5):219–224. [PubMed: 15506703]
5. Palumbo G. Photodynamic therapy and cancer: a brief sightseeing tour. Expert Opinion on Drug Delivery. 2007; 4(2):131–148. [PubMed: 17335411]
6. Hwang JY, Wachsmann-Hogiu S, Ramanujan VK, Nowatzyk AG, Koronyo Y, Medina-Kauwe LK, Gross Z, Gray HB, Farkas DL. Multimodal wide-field two-photon excitation imaging: characterization of the technique for in vivo applications. Biomedical Optics Express. 2011; 2(2): 356–364. [PubMed: 21339880]
7. Agadjanian H, Weaver JJ, Mahammed A, Rentsendorj A, Bass S, Kim J, Dmochowski IJ, Margalit R, Gray HB, Gross Z, Medina-Kauwe LK. Specific delivery of corroles to cells via noncovalent conjugates with viral proteins. Pharm Res. 2006; 23(2):367–377. [PubMed: 16411149]
8. Agadjanian H, Ma J, Rentsendorj A, Valluripalli V, Hwang JY, Mahammed A, Farkas DL, Gray HB, Gross Z, Medina-Kauwe LK. Tumor detection and elimination by a targeted gallium corrole. Proc Natl Acad Sci U S A. 2009; 106(15):6105–6110. [PubMed: 19342490]
9. Pohlmann PR, Mayer IA, Mernaugh R. Resistance to Trastuzumab in Breast Cancer. Clin Cancer Res. 2009; 15(24):7479–7491. [PubMed: 20008848]
10. Yamashiro H, Toi M. Molecular targeted therapy for breast cancer treatment, challenge to cure. Nippon Rinsho. 2010; 68(10):1854–1858. [PubMed: 20954329]
11. Wilken JA, Maihle NJ. Primary trastuzumab resistance: new tricks for an old drug. Annals of the New York Academy of Sciences. 2010; 1210:53–65. [PubMed: 20973799]

12. Chung A, Karlan S, Lindsley E, Wachsmann-Hogiu S, Farkas DL. In vivo cytometry: a spectrum of possibilities. Cytometry A. 2006; 69(3):142–146. [PubMed: 16479602]
13. Zochowski M, Wachowiak M, Falk CX, Cohen LB, Lam YW, Antic S, Zecevic D. Imaging membrane potential with voltage-sensitive dyes. The Biological Bulletin. 2000; 198(1):1–21. [PubMed: 10707808]
14. Scaduto RC Jr. Grotyohann LW. Measurement of mitochondrial membrane potential using fluorescent rhodamine derivatives. Biophysical Journal. 1999; 76(1 Pt 1):469–477. [PubMed: 9876159]
15. Murant RS, Gibson SL, Hilf R. Photosensitizing effects of Photofrin II on the site-selected mitochondrial enzymes adenylate kinase and monoamine oxidase. Cancer Research. 1987; 47(16): 4323–4328. [PubMed: 3038310]
16. Salet C. Hematoporphyrin and hematoporphyrin-derivative photosensitization of mitochondria. Biochimie. 1986; 68(6):865–868. [PubMed: 3019436]
17. Kawai H, Suzuki T, Kobayashi T, Mizuguchi H, Hayakawa T, Kawanishi T. Simultaneous imaging of initiator/effector caspase activity and mitochondrial membrane potential during cell death in living HeLa cells. Biochimica et Biophysica Acta. 2004; 1693(2):101–110. [PubMed: 15313012]

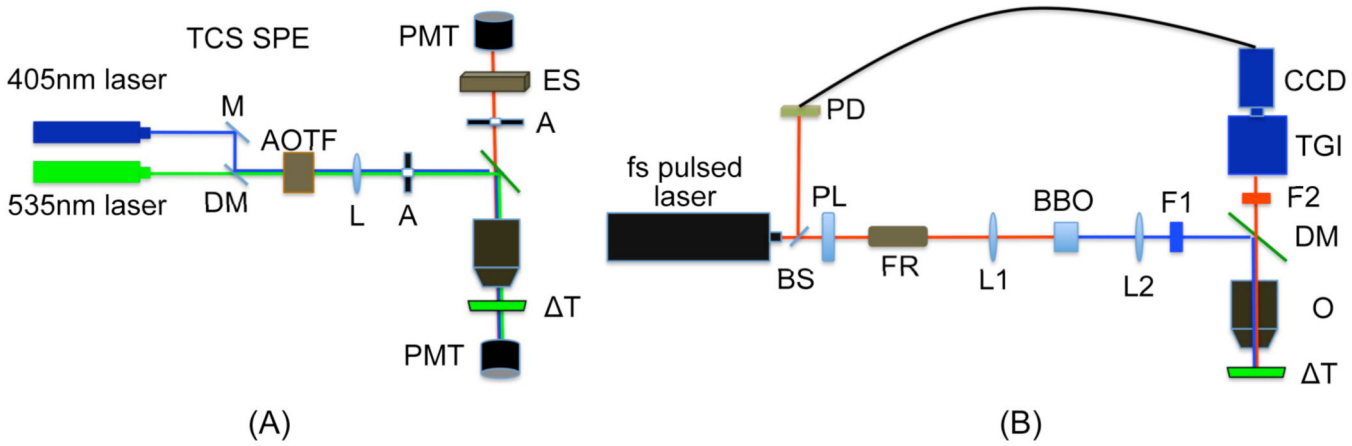

Fig. 1. Experimental setup for multimode optical imaging

(A) confocal/bright-field/spectral imaging system (B) fluorescence lifetime imaging system. M: mirror, DM: dichroic mirror, AOTF: Acousto-optic tunable filters, L: tube lens, A: aperture, ES: light wavelength selector, PMT: photomultiplier tube, ΔT: delta T chamber, PL: polarizer, BS: beam sampler, PD: photodiode detector, FR: faraday rotator, L1, 2: doublet lens (focal lens: 15mm), BBO: beta barium borate crystal, F1: excitation filter (425±5nm), F2: emission filter (610nm±60nm), O: objective, TGI: time-gated intensifier, and CCD: charge-coupled detector. This figure was modified from the experimental setup reported previously [Jae Youn Hwang et al., submitted for publication].

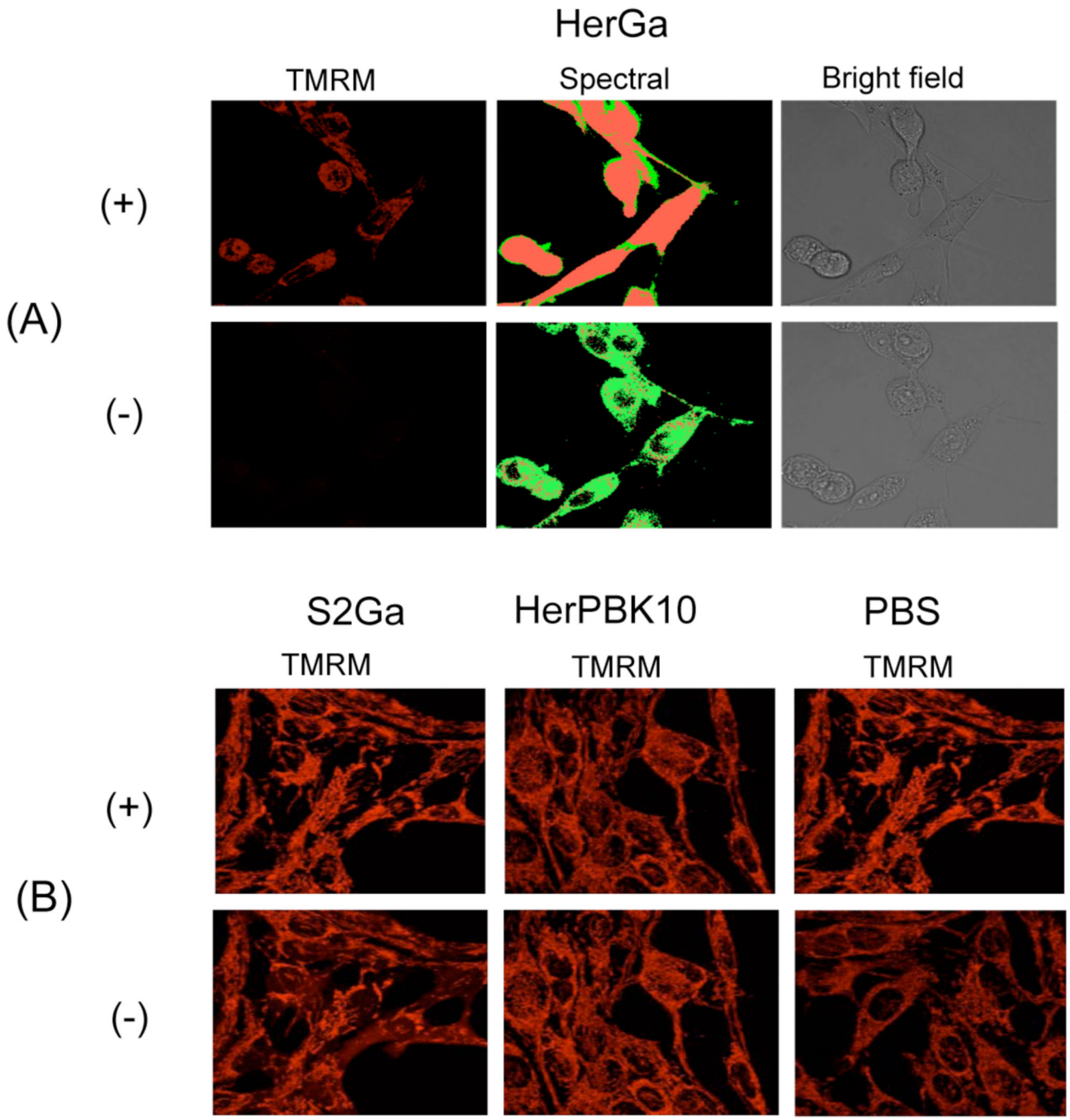

Fig. 2. Mitochondrial membrane potential variation of cells treated with HerGa, HerPBK10, S2GA, or PBS -/+ light exposure

(A) Confocal images of HerGa treated cell -/+ light (450nm–490nm, 17J/cm^2). Left, TMRM fluorescence; Middle, spectral classified images. Red: TMRM. Green: HerGa. Right, bright field images (B) confocal TMRM fluorescence images of S2Ga, HerPBK10, and PBS treated cells -/+ light (450nm–490nm, 17J/cm^2).

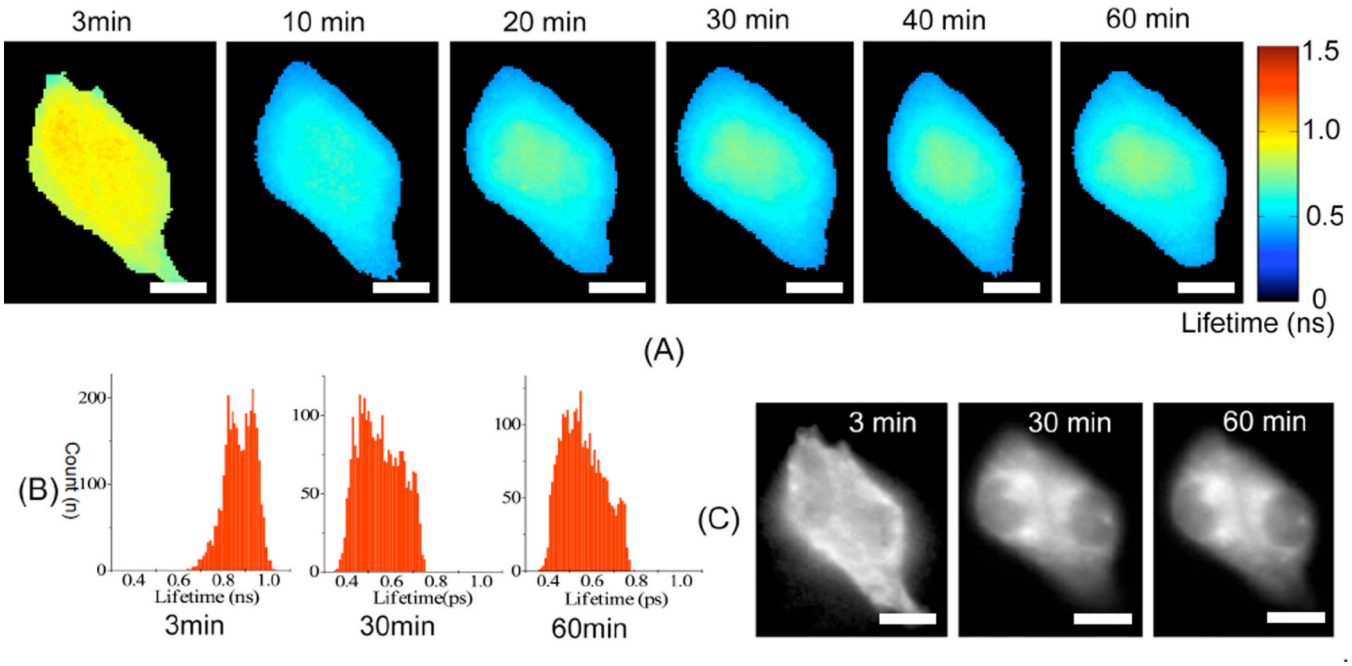

Fig. 3. Fluorescence lifetime changes of HerGa during the uptake

(A) fluorescence lifetime images of HerGa at the indicated time-points (B) histogram of fluorescence lifetime images (C) fluorescence intensity images. Scale bar: 5μm